

Experimental demonstration of a reconfigurable silicon thermo-optical device based on spectral tuning of ring resonators for optical signal processing

William S. Fegadolli,^{1,2,3,*} Liang Feng,^{1,4} Muhammad Mujeeb-U-Rahman,¹ José E. B. Oliveira,² Vilson R. Almeida,^{2,3} and Axel Scherer¹

¹Department of Physics and Electrical Engineering, California Institute of Technology - Caltech, Pasadena, California, USA

²Department of Electronics Engineering, Instituto Tecnológico de Aeronáutica – ITA, Brazil

³Division of Photonics, Instituto de Estudos Avançados – IEAv, Brazil

⁴Department of Electrical Engineering, The State University of New York at Buffalo, Buffalo, New York, USA

*fegadolli@caltech.edu

Abstract: We have experimentally demonstrated a reconfigurable silicon thermo-optical device able to tailor its intrinsic spectral optical response by means of the thermo-optical control of individual and uncoupled resonant modes of micro-ring resonators. Preliminary results show that the device's optical response can be tailored to build up distinct and reconfigurable logic levels for optical signal processing, as well as control of overall figures of merit, such as free-spectral-range, extinction ratio and 3dB bandwidth. In addition, the micro-heaters on top of the ring resonators are able to tune the resonant wavelength with efficiency of 0.25 nm/mW within a range of up to 10 nm, as well as able to switch the resonant wavelength within fall and rise time of 15 μ s.

©2014 Optical Society of America.

OCIS codes: (130.3120) Integrated optics devices; (130.7408) Wavelength filtering devices; (160.6840) Thermo-optical materials.

References and links

1. L. Pavesi and G. Guillot, *Optical Interconnects - The Silicon Approach* (Springer-Verlag, Heidelberg, 2006).
2. M. Lipson, "Guiding, modulating and emitting light on silicon - Challenges and opportunities," *J. Lightwave Technol.* **23**(12), 4222–4238 (2005).
3. V. R. Almeida, R. R. Panepucci, and M. Lipson, "Nanotaper for compact mode conversion," *Opt. Lett.* **28**(15), 1302–1304 (2003).
4. Q. Xu, B. Schmidt, S. Pradhan, and M. Lipson, "Micrometre-scale silicon electro-optic modulator," *Nature* **435**(7040), 325–327 (2005).
5. M. Liu, X. Yin, E. Ulin-Avila, B. Geng, T. Zentgraf, L. Ju, F. Wang, and X. Zhang, "A graphene-based broadband optical modulator," *Nature* **474**(7349), 64–67 (2011).
6. D. J. Thomson, F. Y. Gardes, Y. Hu, G. Mashanovich, M. Fournier, P. Grosse, J.-M. Fedeli, and G. T. Reed, "High contrast 40Gbit/s optical modulation in silicon," *Opt. Express* **19**(12), 11507–11516 (2011).
7. D. T. H. Tan, P. C. Sun, and Y. Fainman, "Monolithic nonlinear pulse compressor on a silicon chip," *Nat Commun* **1**(8), 116 (2010).
8. T. Barwicz, M. A. Popović, M. R. Watts, P. T. Rakich, E. P. Ippen, and H. I. Smith, "Fabrication of add-drop filters based on frequency-matched microring resonators," *J. Lightwave Technol.* **24**(5), 2207–2218 (2006).
9. W. S. Fegadolli, J. E. B. Oliveira, V. R. Almeida, and A. Scherer, "Compact and low power consumption tunable photonic crystal nanobeam cavity," *Opt. Express* **21**(3), 3861–3871 (2013).
10. M. Erdmanis, L. Karvonen, A. Säynätjoki, X. Tu, T. Y. Liow, Q. G. Lo, O. Vänskä, S. Honkanen, and I. Tittonen, "Towards broad-bandwidth polarization-independent nanostrip waveguide ring resonators," *Opt. Express* **21**(8), 9974–9981 (2013).
11. A. W. Fang, H. Park, O. Cohen, R. Jones, M. J. Paniccia, and J. E. Bowers, "Electrically pumped hybrid AlGaInAs-silicon evanescent laser," *Opt. Express* **14**(20), 9203–9210 (2006).
12. X. Sun, A. Zadok, M. J. Shearn, K. A. Diest, A. Ghaffari, H. A. Atwater, A. Scherer, and A. Yariv, "Electrically pumped hybrid evanescent Si/InGaAsP lasers," *Opt. Lett.* **34**(9), 1345–1347 (2009).

13. W. S. Fegadolli, S. H. Kim, P. A. Postigo, and A. Scherer, "Hybrid single quantum well InP/Si nanobeam lasers for Silicon Photonics," *Opt. Lett.* **38**(22), 4656–4658 (2013).
14. T. Creazzo, E. Marchena, S. B. Krasulick, P. K. L. Yu, D. V. Orden, J. Y. Spann, C. C. Blivin, L. He, H. Cai, J. M. Dallesasse, R. J. Stone, and A. Mizrahi, "Integrated tunable CMOS laser," *Opt. Express* **21**(23), 28048–28053 (2013).
15. T. Yin, R. Cohen, M. M. Morse, G. Sarid, Y. Chetrit, D. Rubin, and M. J. Paniccia, "31 GHz Ge n-i-p waveguide photodetectors on Silicon-on-Insulator substrate," *Opt. Express* **15**(21), 13965–13971 (2007).
16. S. Sahni, X. Luo, J. Liu, Y. H. Xie, and E. Yablonovitch, "Junction field-effect-transistor-based germanium photodetector on silicon-on-insulator," *Opt. Lett.* **33**(10), 1138–1140 (2008).
17. S. Assefa, F. Xia, and Y. A. Vlasov, "Reinventing germanium avalanche photodetector for nanophotonic on-chip optical interconnects," *Nature* **464**(7285), 80–84 (2010).
18. F. Xia, T. Mueller, Y. M. Lin, A. Valdes-Garcia, and P. Avouris, "Ultrafast graphene photodetector," *Nat. Nanotechnol.* **4**(12), 839–843 (2009).
19. I. Goykhman, B. Desiatov, J. Khurgin, J. Shappir, and U. Levy, "Locally oxidized silicon surface-plasmon Schottky detector for telecom regime," *Nano Lett.* **11**(6), 2219–2224 (2011).
20. L. Feng, Y. L. Xu, W. S. Fegadolli, M. H. Lu, J. E. B. Oliveira, V. R. Almeida, Y. F. Chen, and A. Scherer, "Experimental demonstration of a unidirectional reflectionless parity-time metamaterial at optical frequencies," *Nat. Mater.* **12**(2), 108–113 (2012).
21. L. Bi, J. Hu, P. Jiang, D. H. Kim, G. F. Dionne, L. C. Kimerling, and C. A. Ross, "On-chip optical isolation in monolithically integrated non-reciprocal optical resonators," *Nat. Photonics* **5**(12), 758–762 (2011).
22. H. Lira, Z. Yu, S. Fan, and M. Lipson, "Electrically driven nonreciprocity induced by interband photonic transition on a silicon chip," *Phys. Rev. Lett.* **109**(3), 033901 (2012).
23. W. S. Fegadolli, V. R. Almeida, and J. E. Oliveira, "Reconfigurable silicon thermo-optical device based on spectral tuning of ring resonators," *Opt. Express* **19**(13), 12727–12739 (2011).
24. C. K. Madsen and G. Lenz, "Optical All-Pass Filters for Phase Response Design with Applications for Dispersion Compensation," *IEEE Photon. Technol. Lett.* **10**(7), 994–996 (1998).
25. W. S. Fegadolli, G. Vargas, X. Wang, F. Valini, L. A. M. Barea, J. E. B. Oliveira, N. Frateschi, A. Scherer, V. R. Almeida, and R. R. Panepucci, "Reconfigurable silicon thermo-optical ring resonator switch based on Vernier effect control," *Opt. Express* **20**(13), 14722–14733 (2012).
26. M. R. Watts, J. Sun, C. DeRose, D. C. Trotter, R. W. Young, and G. N. Nielson, "Adiabatic thermo-optic Mach-Zehnder switch," *Opt. Lett.* **38**(5), 733–735 (2013).
27. A. H. Atabaki, A. A. Eftekhar, S. Yegnanarayanan, and A. Adibi, "Sub-100-nanosecond thermal reconfiguration of silicon photonic devices," *Opt. Express* **21**(13), 15706–15718 (2013).
28. P. Dong, W. Qian, H. Liang, R. Shafiiha, D. Feng, G. Li, J. E. Cunningham, A. V. Krishnamoorthy, and M. Asghari, "Thermally tunable silicon racetrack resonators with ultralow tuning power," *Opt. Express* **18**(19), 20298–20304 (2010).
29. A. H. Atabaki, E. Shah Hosseini, A. A. Eftekhar, S. Yegnanarayanan, and A. Adibi, "Optimization of metallic microheaters for high-speed reconfigurable silicon photonics," *Opt. Express* **18**(17), 18312–18323 (2010).

1. Introduction

Silicon photonics has been considered a promising technology owing to its intrinsic characteristic of allowing high integration of optical devices in small footprints, as well as to its synergy with existing CMOS (Complementary Metal-Oxide-Semiconductor) processes. The applications have promised to cover a wide spectrum, comprising conventional long-distance down to intra-chip communications [1, 2].

For the past decade, several research groups have demonstrated essential building blocks to process optical signals, for example: efficient and broadband input/output coupling systems from optical fibers to optical waveguides [3], high-speed electro-optic modulators [4–6], chip-scale ultrafast pulse compressor [7], tunable filters [8,9], polarization-independent devices [10], heterogeneous integration on silicon-on-insulator (SOI) to produce light sources and photodetectors [11–19], as well as unidirectional [20] and nonreciprocal devices [21, 22], amongst others.

Nowadays, one particular challenge of highly importance in telecommunications has been highly discussed by the technical community; it consists on the development of reconfigurable devices to allow a degree of freedom on optical signal processing and then allow the development of intelligent networks with higher performance.

In this letter, we experimentally demonstrate a reconfigurable silicon thermo-optical filter based on spectral tuning of separate ring resonators; this approach was previously reported on

a theoretical ground in our previous work [23], where its principle of operation was named as the *Persiana* effect [23].

The proposed device consists of a series of uncoupled ring resonators, which in turn are coupled to the same bus waveguide [24] and integrated with micro-heaters atop [23], as shown in Fig. 1. The principle of operation of the device is based on the tuning of the resonance of each ring resonator to tailor the device's optical response, as desired, by means of thermo-optical effect induced by the individual control of the micro-heaters atop of each ring resonator [23]. It is worth pointing out that a detailed analysis of the device was presented in our previous work [23], where we identified optimal theoretical parameters for particular applications.

2. Fabrication

Initially, we optimistically tried to fabricate the device on the grounds of the theoretical design, which was validated by FDTD in our previous work [23]. However we faced two experimental limitations: i) imprecision on the fabrication process, mostly owing to imperfections of E-Beam lithography, side wall roughness caused by Etch and imperfections caused by PECVD deposition, which generated overall random deviation of the optical length of the ring resonator within a range from 4nm to 38nm instead of the required precision (2nm); and ii) we experimentally observed that the micro-heater with radii of approximately 5 μ m melted down before providing enough required shift of the resonant mode to demonstrate the “*Persiana* effect” [23].

The imprecision of the fabrication process in our ring resonator is limited by the capabilities of our facilities but we experimentally adjusted the fabrication parameters of micro-heaters to support a higher shift before melting down and allow us to compensate the intrinsic fabrication deviation by applying a bias current and tune the resonant wavelength on the desired wavelength.

Therefore, the present device structure was slightly redesigned to overcome these experimental limitations not predicted in the previous report [23]. We modified the design parameters as follows: 10 uncoupled identical Si micro-ring resonators are spatially separated and connected to the same Si bus waveguide (Fig. 1). The gap distance between the micro-ring resonators and the bus waveguide is 250 nm; the radius of the ring resonators is 10 μ m; the width and the height of the bus waveguide and ring resonators are 400 nm and 220 nm, respectively; and the widths of the heaters atop of the ring resonators are all set to be 2.5 μ m, similar to the parameter used in our previous works [9, 25].

The device was fabricated by means of two distinct layers: the optical layer and the thermal layer. The optical layer was fabricated using direct E-beam lithography over a SOI substrate with negative-tone E-beam resist (HSQ), followed by dry etch using a mixture of C₄F₈ and SF₆ to form the ten ring resonators and the bus waveguide. Next, a thick layer of 1.5 μ m of silicon dioxide was deposited on the sample using plasma-enhanced chemical vapor deposition (PECVD). The purpose of this oxide layer is not only to make the optical mode symmetric, but also to optically isolate the optical layer from the metal layer, required by the micro-heaters. This isolation helps to avoid absorption loss from metal layer, for both light propagating inside ring resonators and the waveguide; however, the oxide layer still allows enough heat transfer from the thermal layer to the optical layer as previously demonstrated [9].

The thermal layer was then built in two steps using aligned photolithography and positive photoresist with an inversion process: the first step consists of photolithography of the micro-heaters on top of the fabricated and passivated ring resonators, followed by 200-nm thick Nichrome deposition and then lift-off; the second step consists of the photolithography for both contact pads and power feed-lines, followed by (5 nm / 270 nm) Ti/Au deposition and, finally, lift-off. Various stages of the fabricated device can be seen in Fig. 1.

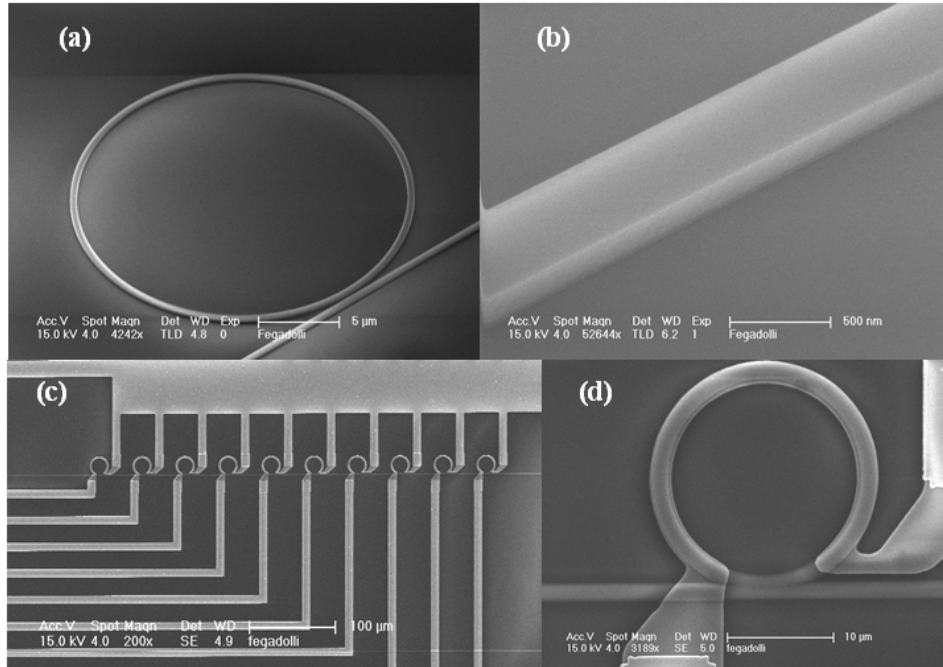


Fig. 1. Scanning electron microscope micrograph of (a) single ring resonator and (b) bus waveguide after exposed and etched; (c) final device passivated with a thermal oxide layer and integrated with micro-heaters and pad contacts atop; and (d) the scaled region of a ring resonator seen in (c).

3. Measurements and results

We began our measurements characterizing the electrical properties of our heaters using a semiconductor analyzer and scanned the electric current versus voltage in order to measure the resistance of our heaters, which was found to be around $700 \, \Omega$. In optical measurements, we used nano-positioners to align and efficiently couple light from lensed optical fibers into the silicon waveguides with inverted nanotapers [3]. An Agilent tunable laser model 81980A was used as light source, and an Agilent fiber-coupled power meter model 81636B was used to measure transmitted signals. A Keithley precision current source model 2400 was used to control the electric current on the micro-heaters for thermo-optical control.

Moreover, we characterized one of the ring resonators in order to obtain the power consumption efficiency and time dependency. The results for the single ring resonator are shown in Fig. 2. Figure 2(a) shows the optical response for different bias current values, Fig. 2(b) shows the resonant wavelength as a function of electric current and electric power, indicating that the ratio of resonant wavelength per electrical power is around $0.25 \, \text{nm/mW}$. In addition to the electrical characterization of the thermo-optical properties of the device, we also investigated the required fall and rise time to switch “on” and “off” the resonance condition for the resonant wavelength; this result is shown in Fig. 2(c) where we observe $15 \, \mu\text{s}$ for the fall and rise times. The electrical power was set to $300 \, \mu\text{W}$.

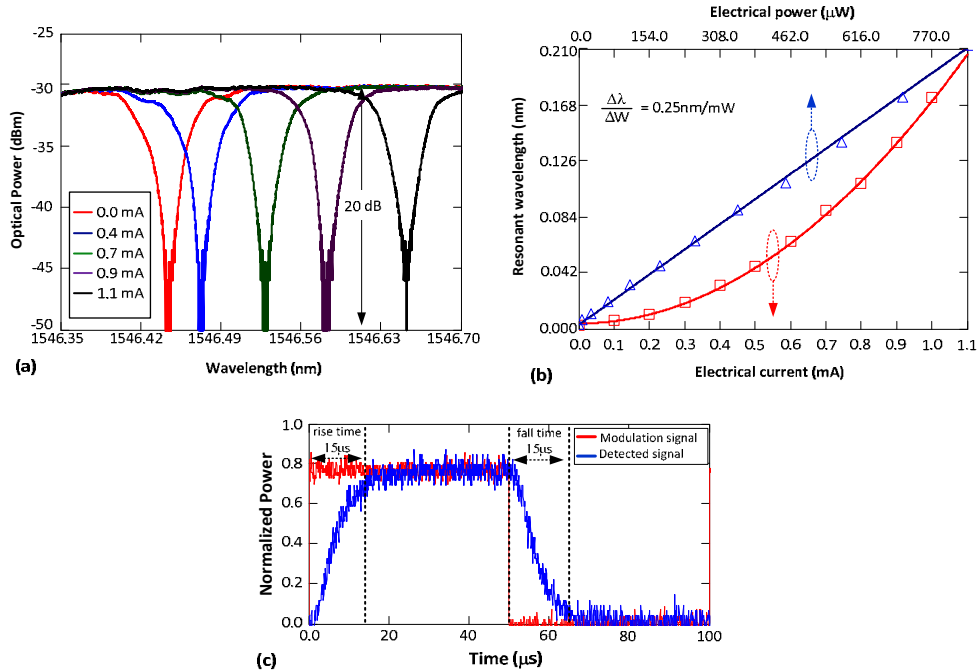


Fig. 2. (a) Optical response of a single ring resonator as a function of the electric current applied to the micro-heaters; (b) resonant wavelength as a function of the electrical power and electric current applied to the micro-heaters. (c) Temporal behavior of the modulation and detected signals

Our micro-heaters were experimentally optimized to provide high resonant shift; however, it is worthy pointing out that there is enough room for further optimization regarding power efficiency and switching speed, as previously demonstrated by other authors [26–29].

Finally, we measured the optical response of the device shown in Fig. 1(c) with and without appropriate bias currents applied to the micro-heaters, as depicted in Fig. 3. Without bias currents, it can be seen that, although all the 10 ring resonators were designed and fabricated to be identical, the randomness in fabrication made all the ring resonators slightly off-resonance among each other and with different extinction ratio, thus resulting in a series of different resonant dips in the transmission spectrum from 1545 nm to 1560 nm.

To compensate the adverse effect from such fabrication randomness, we applied distinct and appropriate bias currents to each one of the micro-heater; the overall dissipated power in the micro-heater to form this optical sintonized state was 132 mW, this condition allows us to flexibly control the thermo-optical blue and red-shifts of each resonant wavelength, and thus reconfigure the entire device as desired to tailor the Free-Spectral-Range (*FSR*), extinction ration, and 3dB bandwidth.

Consequently, we successfully realized all the resonances from different ring resonators to coincide at the same wavelength, behaving like 10 identical micro-ring resonators in terms of optical length (not with same figure of merit). This condition is referred as “Level 0” [23].

Figure 3 (b) shows a comparison between the optical response vs. normalized wavelength of a single resonator and all the ten ring resonators tuned at the same wavelength in order show the increasing of bandwidth, we compared when all resonant modes are tuned at the same wavelength with a single resonant mode from our best ring resonator. Because of the cascaded effect, the extinction ratio of the resonance becomes larger compared to those without bias currents (increasing of 10 dB) and the 3dB bandwidth is increased by approximately 10 times the value of a single ring resonators.

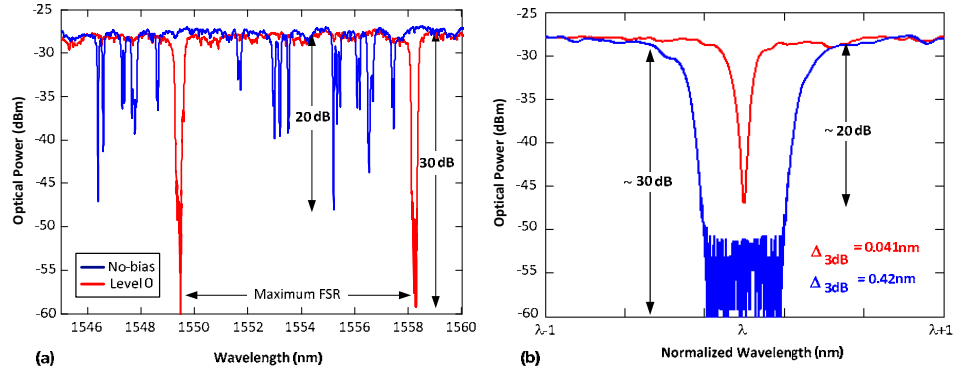


Fig. 3. (a) Optical response of the device in transmission under two conditions: no bias current applied, and appropriate bias currents applied such that the “Level 0” was established. (b) Extinction ratio and bandwidth comparison between a sing ring resonator and *Persiana* structure properly biased.

To realize the *Persiana* effect based on Level 0, we focused on the resonance dip located around the wavelength of 1558 nm in Fig. 3. Based on the bias current condition on Level 0, we applied additional sets of electric current values to the heaters atop the ring resonators, which were classified into two separate groups: additional + 4 mW (overall power) are applied on heaters for the first five ring resonators, creating a red shift of the resonance dip, while −4 mW (overall power) are applied on the last five ring resonators, causing a blue shift of the resonance dip. This condition is called Level 1 [23]. Therefore, instead of one single resonance observed on Level 0 (Fig. 4), the overall resonance spectrum splits into two, demonstrating the expected *Persiana* effect, as shown in Fig. 4(a), in which the transmission spectra for the quasi-TE₀₀ polarization state is plotted. In addition, Fig. 4(b) shows the extinction ratio between both levels as a function of the wavelength.

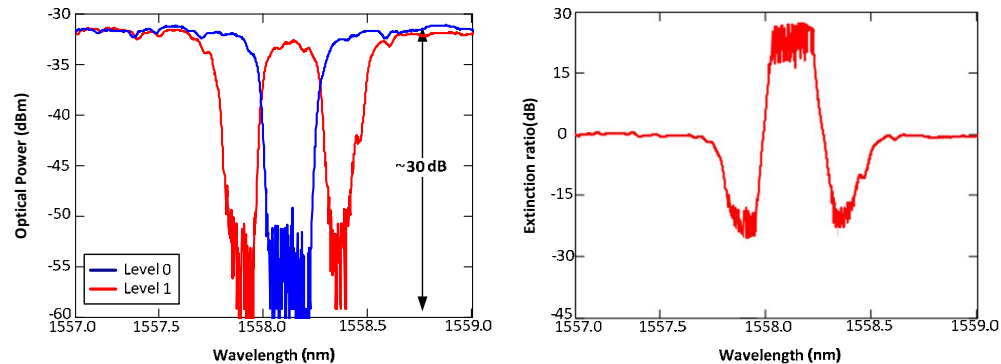


Fig. 4. (a) Optical response of the device operating on Levels 0 and 1, (b) extinction ration as a function of wavelength.

It is worth pointing out that no thermal crosstalk was observed in the measurements and it is evident that the transmission spectrum of the device can be reconfigurable and desirably tailored, as well as the corresponding optical signal can be efficiently filtered or slowly modulated thermo-optically between Level 0 and Level 1. The extinction ratio modulation can be as high as 30 dB, as shown in Fig. 4 and the overall Free-Spectral-Range (FSR) can be tailored accordingly.

Conclusion

In summary, we have experimentally demonstrated a reconfigurable Si thermo-optical device able to tailor its spectral optical response, allowing several degrees of reconfigurable control, such as *FSR*, bandwidth, extinction ratio, and spectral shape. The device brings unique functionalities on optical signal processing that may open the doors for fundamental applications on the next generation of intelligent and reconfigurable networks.

Acknowledgment

Authors thank the NSF CIAN ERC (Grant EEC-0812072), CAPES and CNPQ (Brazilian Foundations) for the financial support and Kavli Nanoscience Institute at Caltech for technical support.